PHYSICAL REVIEW D **93,** 053007 (2016)

Bounds on neutrino-scalar Yukawa coupling

P. S. Pasquini[1,2,*] and O. L. G. Peres[1,3,†]

[1]*Instituto de Física Gleb Wataghin, UNICAMP, 13083-859, Campinas São Paulo, Brazil*
[2]*AHEP Group, Institut de Física Corpuscular - C.S.I.C./Universitat de València, Parc Cientific de Paterna. C/Catedratico José Beltrán, 2 E-46980 Paterna (València), Spain*
[3]*Abdus Salam International Center for Theoretical Physics, Strada Costiera 11, 34014 Trieste, Italy*

(Received 9 November 2015; published 9 March 2016)

General neutrino-scalar couplings appear in many extensions of the Standard Model. We can probe these neutrino-scalar couplings by a leptonic decay of mesons and from a heavy neutrino search. Our analysis improves the present limits to $|g_e|^2 < 1.9 \times 10^{-6}$ and $|g_\mu|^2 < 1.9 \times 10^{-7}$ at 90% C.L. for massless scalars. For massive scalars, we found for the first time the constraints for g_α^2 couplings to be $10^{-6} - 10^{-1}$, respectively, for scalar masses between up 100 MeV, and we have no limits for masses above 300 MeV.

DOI: 10.1103/PhysRevD.93.053007

I. INTRODUCTION

Although in the Standard Model there are no couplings between neutrinos and scalar fields due to the nonexistence of right-handed neutrino fields, many of its extension contains an enlarged scalar sector that may result in nonuniversal Yukawa interactions that couples neutrinos and those new scalars.

Nonuniversal neutrino-scalar couplings can have interesting consequences such as: (i) existence of new decay channels for particle decays, especially meson decays and lepton decays [1,2], (ii) induced neutrino decay [3–7], (iii) the presence of new channels for the energy loss of supernovae caused by an enhanced emission of neutrinos and scalars χ [8], (iv) new channels for a neutrinoless double β decay with the emission of massless χ in the final state [9], and (v) a change in flavor ratios of high energy neutrinos from astrophysical sources [10,11].

In general, we can parametrize the neutrino-scalar Lagragian to be

$$-\mathcal{L} = \frac{1}{2} g_{AB} \bar{\nu}_A \nu_B \chi_1 + \frac{i}{2} h_{AB} \bar{\nu}_A \gamma_5 \nu_B \chi_2, \tag{1}$$

where χ_1 (χ_2) is the hypothetical scalar (pseudoscalar), the ν_A are the neutrinos, which may or may not have a right-handed part, and the coupling constant g_{AB} (h_{AB}), where A, B runs over two possible basis: (i) $A, B =$ Greek index: neutrino flavor eigenstates e, μ, and τ, and (ii) $A, B =$ Roman index: neutrino mass eigenstates 1,2, and 3, that are related by,

$$g_{ij} = U^*_{i\alpha} U_{\beta j} g_{\alpha\beta}, \tag{2}$$

and equivalently, for h.

Most modern experiments that can probe neutrino-scalar interaction cannot distinguish between neutrino final states, so it is convenient to define an effective coupling constant squared:

$$|g_l|^2 \equiv \sum_\alpha (|g_{l\alpha}|^2 + |h_{l\alpha}|^2) \tag{3}$$

with $\alpha, l = e, \mu, \tau$, where U is the mixing matrix of the three lightest neutrinos.

Previous constraints on these couplings are $|g_e|^2 < 4.4 \times 10^{-5}$, $|g_\mu|^2 < 3.6 \times 10^{-4}$, and $|g_\tau|^2 < 2.2 \times 10^{-1}$ at 90% C.L. and were obtained from meson as well as from lepton decays analysis [2].

For the absence of detection of neutrinoless double β decay, it was found that $|g_e|^2 < (0.8\text{–}1.6) \times 10^{-5}$ at 90% C.L. [9], where the uncertainties came from the computation of nuclear matrix elements of the neutrinoless double β decay. All these limits were made in the limit of massless scalar field χ.

The effective Lagrangian for neutrino-scalar couplings shown in Eq. (1) can be embedded in different extensions of the Standard Model. The general trend is to have the inclusion of new scalar particles in different representations with nonuniversal couplings between the different families and also the addition of new sterile neutrino states. For instance, Ref. [11] presents a model with a $\mathrm{SU(3)_c} \otimes \mathrm{SU(2)_L} \otimes \mathrm{U(1)_Y} \otimes \mathrm{U(1)_H}$ symmetry that included as new fields one extra singlet scalar boson and three right-handed neutrinos. Another example is the model with a $\mathrm{SU(3)_c} \otimes \mathrm{SU(3)_L} \otimes \mathrm{U(1)_N}$ symmetry that due to an anomaly cancellation requirement has already nonuniversal couplings [12]. Recently, a lot of theoretical models with scalars that have vacuum expectation values (vev) that are significantly smaller then the vev of the Standard Model Higgs, $v_{\mathrm{SM}} = 246$ GeV were proposed. Examples of these models involve neutrophilic scalars as in Ref. [13] with vev ~eV and models with gauged B-L symmetry [14,15] that also have vev much smaller than the SM vev resulting in small scalar masses, ranging from eV to TeV values.

*pasquini@ifi.unicamp.br
†orlando@ifi.unicamp.br

This opens an interesting point to study the consequences of nonuniversal neutrino-scalar couplings for massive scalar fields χ that have not been studied so far. Then our goal is to revisit the bounds on neutrino-scalar couplings for massless scalars and to compute the bounds on the neutrino with light *massive* scalars.

Notice that $\chi_{1,2}$ are not the SM Higgs field for an analysis of the consequences of the Higgs coupling to neutrinos, see [16]. Also, the interaction between the neutrino scalar may or may not be reminiscent of a neutrino mass generating mechanism, this has to be analyzed case by case.

This paper is organized as follows. In Sec. II, we discuss the computation of meson decay when we have nonuniversal neutrino-scalar couplings, then in Sec. III, we discuss the available data for meson decay rate and spectrum. In Sec. IV, we made the analysis and extract the constraints on the neutrino-scalar couplings. In Sec. V, we translated the bounds on the mass basis, and we conclude in Sec. VI summarizing our main results.

II. BOUNDS USING MESON DECAY

The leptonic decay rate of a meson P, $P \to l + \bar{\nu}_l$ at three level is given by

$$\Gamma^0(P \to l\nu_l) = \frac{G_F^2 f_P^2 |V_{qq'}|^2 m_P^3}{8\pi}(x_l + \alpha - (x_l - \alpha)^2) \times \lambda^{1/2}(1, x_l, \alpha), \tag{4}$$

where $x_l = (\frac{m_{\nu_l}}{m_P})^2$ and $\alpha = (\frac{m_l}{m_P})^2$, where m_{ν_l} is the neutrino mass and m_l is the lepton mass, G_F is the Fermi constant, f_P the meson decay constant, $V_{qq'}$ is the corresponding CKM-matrix element of the decay, and $\lambda(x, y, z)$ is the well-known kinematic triangular function [17].

Precise branching ratio measurements of mesons open a window to probe the scalar interaction due to the fact that it is chiral suppressed, e.g., for massless neutrinos, $m_{\nu_l} \to 0$, the total rate is proportional to $\alpha \propto m_l$ and is very small when $m_P \gg m_l$.

The precision of π and K meson decay rate requires also the inclusion of electromagnetic and weak radiative corrections that can be parametrized as follows:

$$\Gamma(P \to l\nu_l) = \Gamma^0(P \to l\nu_l) S_{EW}(1 + \alpha_{el} G_{rad}). \tag{5}$$

The electromagnetic radiative corrections G_{rad} came from short and long range corrections and were computed for pions in Ref. [18] at one loop level and at 2 loop level for pions and kaons in Ref. [19]. A nice review of these computations can be found in Ref. [20]. The electroweak radiative corrections S_{EW} are given in Ref. [18].

When we add the interaction from nonuniversal neutrino-scalar couplings shown in Eq. (1), the meson have a three body decay

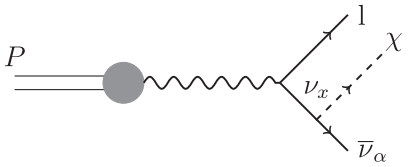

FIG. 1. Tree level Feynman diagram of the three-body decay.

$$P \to l + \bar{\nu}_\alpha + \chi, \tag{6}$$

where the Feynman diagram is given by Fig. 1. The rate was computed in Ref. [1]. The differential rate for this process is

$$d\Gamma(P \to l\nu_\alpha\chi) = \Gamma(P \to l\nu_x) dR, \tag{7}$$

where the rate $\Gamma(P \to l\nu_x)$ is similar to the two-body rate of Eq. (4) replacing the mass of the real neutrino of the two body decay in the final state ν_l by a virtual neutrino ν_x of an invariant mass $m_{\nu_x}^2$ as shown in Fig. 1. The rate $\Gamma(P \to l\nu_x)$ is given by

$$\Gamma(P \to l\nu_x) = \frac{G_f^2 f_p^2 |V_{qq'}|^2 m_P^3}{8\pi}(x + \alpha - (x - \alpha)^2) \times \lambda^{1/2}(1, x, \alpha), \tag{8}$$

where we made the replacement $x_l \to x = (\frac{m_{\nu_x}}{m_P})^2$ in Eq. (4). To obtain the full rate of the three body decay, we should integrate over all possible invariant mass m_{ν_x} of the virtual neutrino whose phase space is not a Dirac delta fixed by energy conservation but it is an additional independent variable. The factor dR in Eq. (7) is as follows:

$$dR = \frac{(x^2 + \beta^2 + 6x\beta - \gamma x - \gamma\beta)\lambda^{1/2}(x, \beta, \gamma)}{(x - \beta)^2 x^2} \frac{|g_{l\alpha}|^2}{32\pi^2} dx, \tag{9}$$

where $\gamma = (\frac{m_\chi}{m_P})^2$, and the m_χ is mass of scalar χ, and $g_{l\alpha}$ is the coupling of the vertex neutrino-neutrino-scalar $\nu_l - \nu_\alpha - \chi$ from Eq. (1). The integration limits are $\gamma \le x \le (1 - \sqrt{\alpha})^2$. Notice that for $\beta, \gamma \to 0$, this integration is infrared (IR) divergent. Previous calculations did not present a formal treatment of this divergence, Ref. [1] assumed $m_\chi, m_\nu \sim 1$ eV, and Ref. [21] took $m_\nu \sim 0.1$ MeV. We present a finite calculation in the Appendix A.

III. LEPTONIC DECAY DATA

The experimental data used in this work comes from various meson decays measurements, shown in Table I. The analysis is subdivided into two groups of data:

(a) The first group comes from rates of leptonic decay of mesons.

TABLE I. Reactions used in this work.

Reaction	Reference
$P \to l\bar{\nu}$ (π, K)	[17]
$P \to l\bar{\nu}$ (D, D_s, B)	[22–26]
$\pi^+ \to e^+\nu_H$	[27]
$K^+ \to \mu^+\nu_H$	[28]
$\mathrm{Br}(\pi^+ \to e^+\nu_e\nu\bar{\nu}) < 5 \times 10^{-6})$	[17]
$\mathrm{Br}(K^+ \to \mu^+\nu_e\nu\bar{\nu}) < 6 \times 10^{-6})$	[17]

(b) The second group is obtained from charged lepton spectrum of mesons decay.

A. Leptonic rates constraints

Assuming zero neutrino mass (or small enough), and that the experiment cannot differentiate between emitted neutrinos, it is possible to write the correction to the decay rate as,

$$\Gamma(P \to \text{Leptonic}) = \Gamma_{\text{SM}} + |g_l|^2\Gamma', \tag{10}$$

where Γ_{SM} is the expected SM contribution to the P-leptonic decay. $|g_l|^2\Gamma'$ represents the contribution of the scalar and pseudoscalar couplings of Eq. (1),

$$|g_l|^2 = \sum_{\alpha=e,\mu,\tau} |g_{l\alpha}|^2 + |g'_{l\alpha}|^2, \tag{11}$$

and Γ' is a numerical factor obtained by integrating Eq. (7) that depends on the particle masses. Notice that if $|g_l|^2 \to 0$, we recover the SM results.

The data from meson leptonic decay for light mesons (π and K) include all available space of a three body decay due to the fact that it is hard to separate $P \to l\nu_l$ and $P \to l\nu_l\gamma$; thus, to obtain the correction Γ', we can safely include an all x integration limit. This makes the ratio $\frac{\Gamma'}{\Gamma_{\text{SM}}}$ reaches orders of 10^2–10^3 due to the chiral suppression that combined with the smallness of the experimental error allow us to put stringent bounds from such decays.

For heavy mesons such as D, D_s, and B, the leptonic decay rate of heavy mesons is suffering from a large background of hadronic decays, and the measurement of meson decay is triggered by the detection of the charged lepton in the final state and a missing four momentum. In the SM, the missing energy comes from the neutrino of the two body decay that we are assuming to be very small, which is equivalent to $M^2_{\text{Miss}} = m^2_{\nu_l} \sim 0$. Nevertheless, experiments can only select leptonic events with $M^2_{\text{Miss}} \lesssim 0.1\ \text{GeV}^2$ due to detector limitations. This opens a window to probe scalar masses different from zero, we can relate the missing energy with the x_l variable $M^2_{\text{Miss}} = x_l m_P^2$ with the SM two-body decay. When we include the three body decay, the relevant variable is x, and we can relate $M^2_{\text{Miss}} = x m_P^2$. Thus, the experimental cut $(M^2_{\text{Miss}})^{\text{max}} \lesssim 0.1\ \text{GeV}^2$ translates to an upper limit in the range of variable x, $\gamma \le x \le x_{\text{max}}$, where $x_{\text{max}} = (M^2_{\text{Miss}})^{\text{max}}/m_P^2$.

TABLE II. Most precise V_{CKM} matrix elements compared to those used here. All of the values comes from the Particle Data Group (PDF) [17].

Element	Most precise	Not from Leptonic decay
$\lvert V_{\text{ud}}\rvert$	…	0.97425(22)
$\lvert V_{\text{us}}\rvert$	0.2253(10)	0.2253(14)
$\lvert V_{\text{cd}}\rvert$	0.225(8)	0.220(12)
$\lvert V_{\text{cs}}\rvert$	0.986(16)	0.953(25)
$\lvert V_{\text{ub}}\rvert$	$4.22(42) \times 10^{-3}$	$4.13(49) \times 10^{-3}$

TABLE III. Form factors f_p from lattice QCD [29].

	f_P [MeV]
π	130.2(1.4)
K	156.3(0.9)
D	209(3.3)
D_s	250(7)
B	186(4)

Two points should be considered when we compare the data from the meson leptonic decay rate and the theoretical predictions: the value of the meson constant f_P and of the CKM elements $|V_{qq'}|^2$. Both quantities usually were obtained from the two-body leptonic decay (see, for example, Ref. [17]), and then if we want to test the two-body for new physics, we cannot use these values. In previous Refs. [1,2], it was decided to use the f_P and $|V_{qq'}|^2$ due to the fact that we cannot extract the constraints to neutrino-scalar couplings without these assumption. In this work, we decided to use the information for f_P and $|V_{qq'}|^2$ from other places in the following way:

(i) Some precise measurements of the CKM matrix elements (D, D_s, and B) comes exactly from the fit of meson leptonic decay rate measurements [17]; thus, those results could be contaminated by exactly the decays we want to find. The solution is to use other measurements of CKM mixing matrix, such as the meson β decay (e.g., $D \to \pi l\nu$) and pay the price of less precise values. Table II compares the most precise values of CKM mixing matrix, and the ones used here that do not come from leptonic decays.

(ii) Meson decay constant, f_P, is also measured from the leptonic decay for light mesons (π and K). Recently, lattice QCD was able to obtain them with good precision, enabling this kind of analysis for the first time. The numerical values of f_P can be found in Ref. [29], and we listed them in Table III.

B. Leptonic spectrum constraints

The second group is obtained from a heavy neutrino search which scans the charged lepton spectrum for peaks of two-body decays. This is the first time that this kind of data is used to restrict neutrino-scalar couplings. We obtain

the best constraints on these couplings from the spectrum analysis.

Inspection of the light meson decay spectrum that was used to search for heavy neutrinos, of mass m_H, by peak search, in special [27,28] found no evidence, putting bounds on the heavy neutrino mass and its mixing matrix to the active neutrinos. The contribution to the charged lepton spectrum can be parametrized on the following form [28]:

$$d\Gamma(P \to l\nu_H) = \rho\Gamma_0 |U_{eH}|^2 \delta(p_{\text{peak}} - p_l) dp_l. \tag{12}$$

With Γ_0 from Eq. (4) setting $m_\nu = 0$, $|U_{eH}|^2$ is the mixing of the heavy neutrino presented in the decay $P \to e + \nu_H$, p_l is the charged lepton momentum. The heavy neutrino mass information is contained only in p_{peak}, the charged lepton momentum expected for a two-body decay of meson P,

$$p_{\text{peak}} = \frac{\lambda^{1/2}(m_P^2, m_l^2, m_H^2)}{2m_P}, \tag{13}$$

and in the variable ρ that is given by

$$\rho = \frac{\sqrt{1 + (\alpha - \beta)^2 - 2(\alpha + \beta)}(\alpha + \beta - (\alpha - \beta)^2)}{\alpha(1 - \alpha)^2}, \tag{14}$$

which is the correction for the two-body meson decay for a heavy neutrino H with mass m_H and $\beta = (\frac{m_H}{m_P})^2$ compared with a massless neutrino limit of Eq. (4).

We can use this information to constrain the neutrino-scalar couplings in the following way. The spectrum with a heavy neutrino should have a peak at a mass of aa heavy neutrino m_H proportional to the mixing of a heavy neutrino $|U_{eH}|^2$ with the electron neutrino (see Fig. 2). The three body decay from the Feynman diagram shown in Fig. 1 has a continuous spectrum shown in Fig. 2 by the dashed, solid, and dotted-dashed curves, respectively, that has numerical values above, equal, and below the maximum values of the spectrum of a heavy neutrino in two body decays. Saying, in other words, we can put a bound by comparing the number of events in peak search area (below the two-body heavy neutrino search) and the three body search. Effectively, the rate of the heavy meson decay given in Eq. (12) has to be equal to the three body decay rate given in Eq. (7):

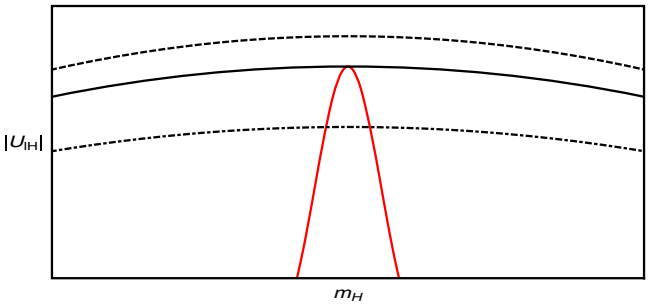

FIG. 2. This plot shows three hypothetical scenarios, the red line represents the peak search, the dashed line a signal, and the dotted-dashed a negative signal, the solid line is the limiting case.

$$|U_{lH}|^2 = \frac{\Gamma(P \to l\nu_x)}{\rho(\alpha, x, \beta)\Gamma_0} \frac{dR}{dp_l}\bigg|_{\beta \to x} \tag{15}$$

and using the constraints from heavy neutrino that constrain the variables $|U_{lH}|^2 \times m_h$ [28], we can get constraints on neutrino-scalar couplings.

IV. ANALYSIS AND RESULTS

We are going to get the bounds from neutrino-scalar couplings for different values of a scalar particle. First, we are going to do the case studied so far in the literature [1,2], when the scalar has zero mass, $m_\chi \to 0$ in Sec. IV A and in the Sec. IV B for the case of $m_\chi \neq 0$.

A. Case I: $m_\chi = 0$

To obtain bounds on the Yukawa coupling constants, we used a χ^2 method, defining it as,

$$\chi^2 = \sum_i \frac{\left(\Gamma_{\text{Teo}}^{(i)} - \Gamma_{\text{Exp}}^{(i)}\right)^2}{\sigma_i^2}, \tag{16}$$

where i runs over the experimental data points. To obtain those bounds, we marginalized all three CKM elements (V_{us}, V_{cd}, V_{cs}) by varying four parameters: $|V_{\text{CKM}}|$'s (and a coupling constant $|g_l|^2$ to find the χ^2_{min}). Our results on $m_\chi = 0$ can be compared with previous bounds found in the literature in Table IV. It is possible to see that in this scenario, the g_τ coupling constant is poorly constrained due to the fact that the errors from the mesons decays and CKM matrix are rather large.

In contrast, the case of assuming the fixed central value of $|V_{\text{CKM}}|$ using the second column of Table II, we can bound it as $|g_\tau|^2 < 8$, which is still bigger than the previous bounds obtained from τ decay [2]. The other coupling constants with fixed CKM are described in red in Table IV.

TABLE IV. Comparison between previous bounds [2,9] with our results with $m_\chi = 0$, using the rates of the meson decay at 90% C.L. In black, the bounds marginalizing V_{CKM}; in red, taking the central value of uncorrelated measurements.

Constants	Ref. [2]	Ref. [9]	Our results
$\|g_e\|^2$	$<4.4 \times 10^{-5}$	$<(0.8\text{–}1.6) \times 10^{-5}$	$<4.4(4.4) \times 10^{-5}$
$\|g_\mu\|^2$	$<3.6 \times 10^{-4}$		$<4.5(3.6) \times 10^{-6}$
$\|g_\tau\|^2$	$<2.2 \times 10^{-1}$		$<40(8)$

TABLE V. Comparison between previous bounds [2,9] with our results at $m_\chi = 0$ with meson decay rate and lepton spectrum from a heavy neutrino search at 90% C.L.

Constants	Ref. [2]	Ref. [9]	Our results
$\lvert g_e\rvert^2$	$<4.4\times10^{-5}$	$<(0.8\text{–}1.6)\times10^{-5}$	$<1.9\times10^{-6}$
$\lvert g_\mu\rvert^2$	$<3.6\times10^{-4}$		$<1.9\times10^{-7}$

Notice that our analysis is more complete than those from the literature that have not taken into account the possible correlation between the measurements from $|V_{\rm CKM}|$ and the bounds on $|g_l|^2$.

From the Eq. (15), we can get the constraints from Refs. [27,28] and translate to bounds on neutrino-scalar couplings.

The data from heavy neutrino search can be used to put bounds on the coupling constants too; all results are summarized in Table V. One can see that a heavy neutrino search is 1 to 3 orders of magnitude more stringent than those from branching ratios, since it takes into account the decay spectrum. The meson decay analysis shows that the SM + scalar has a minimum $\Delta\chi^2$ for $|g_l|^2 \neq 0$, which can be seen for $l = e$ case in Fig. 3. Thus, to evaluate whether or not the SM + scalar with $|g_l|^2 \neq 0$ is a better model than assuming only the SM, we compared both situations by using Bayesian inference taking the prior as a normalized Gaussian distribution around each experimental point as evidence p,

$$p(g|\text{data}, M_{\text{SM}+\chi}) = Ne^{-\frac{1}{2}\chi^2(g^2)} \tag{17}$$

then using the Bayes factor, which can be defined as [30]

$$B = \frac{p(d|M_{\text{SM}})}{p(d|M_{\text{SM}+\chi})} = \frac{p(g^2|d, M_{\text{SM}+\chi})}{p(g^2|M_{\text{SM}+\chi})}\bigg|_{g^2=0}, \tag{18}$$

we can compare the models by calculating B: (I) if $B \ll 1$, the model with more parameters is favored over the model with less parameters, on the other hand, (II) if $B \gg 1$, the model with less parameters is favored due to the description

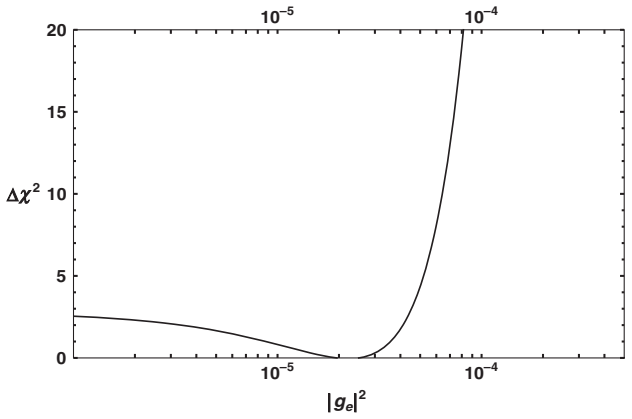

FIG. 3. Marginalized $\Delta\chi^2$ as a function of the value of $|g_e|^2$.

TABLE VI. Bayes Factor of SM + scalar over SM.

Parameter	$\ln[B]$
$\lvert g_e\rvert^2$	5.7
$\lvert g_\mu\rvert^2$	7.2
$\lvert g_\tau\rvert^2$	1.5

of the data. (III) If $B \approx 1$, the data points do not contribute significantly to distinguish between both models. The last equality in Eq. (18) is true when the model M_χ has one extra parameter, g compared to $M_{\rm SM}$ and reduces to the same results when $g^2 = 0$. Then, $p(g^2|d, M)$ is the probability of the value g^2 of the parameter given the data points and assuming M true, and $p(g^2|M)$ is the probability distribution of g^2 in the model, in this case, $p(g^2|M_\chi) = (4\pi)^{-1}$ for $\frac{g^2}{4\pi} < 1$ and zero otherwise. We have found the B values for $|g_i|^2 \neq 0$, and we have shown it in Table VI. For the three couplings constants, the preference of SM + scalar model over the SM is less then 2σ away and from this, we conclude there is no stronger preference for $|g_i|^2 \neq 0$.

B. Case II: $m_\chi \neq 0$

This case was never studied and corresponds to the general case when $m_\chi \neq 0$. We proceeded similarly with Sec. IV A, but using the central value from Table II for the CKM mixing elements and thus, using Eq. (9). Now we have two independent variables from the neutrino-scalar lagrangian, the m_χ and the couplings $|g_l|^2$ as defined in Eq. (11). Our results are shown in Figs. 4,5, and 6, respectively, for $|g_e|^2$, $|g_\mu|^2$, and $|g_\tau|^2$ for the constraints from the rate of leptonic meson decay and the lepton spectrum, respectively, in the green and yellow curves at 90% C.L. Notice that in both cases $|g_e|^2$ and $|g_\mu|^2$, the

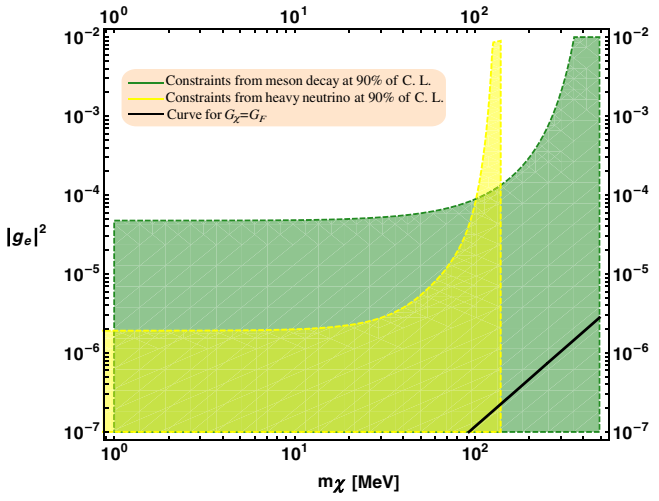

FIG. 4. Bounds on $|g_e|^2$ versus m_χ. The blue curve comes from heavy neutrino and the red curve comes from meson decay at 90% C.L.

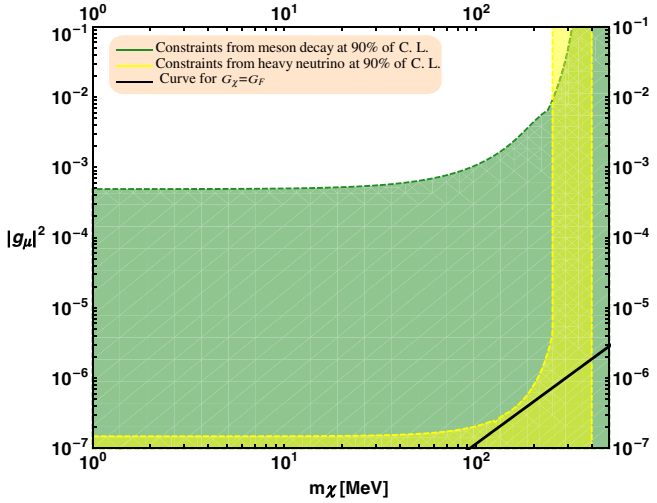

FIG. 5. Bounds on $|g_\mu|^2$ versus m_χ. The yellow curve comes from heavy neutrino search in lepton spectrum and the green curve comes from rate of meson decay at 90% C.L.

bounds can be assumed to be constant up to masses of an order of ∼200 MeV and ∼100 MeV, respectively. The constraints for $|g_\tau|^2$ are weaker due to low statistics of experimental data and also, the larger is the lepton mass, the less effective is the chiral suppression of the two-body meson decay. To have an intuitive idea of the size of our constraints, for the case of $m_\chi \neq 0$, we can compare the strength of a neutrino-scalar interaction represented by $G_\chi \equiv |g_l|^2/m_\chi^2$, $l = e, \mu, \tau$ with the strength of the weak interaction G_F. They are equal when

$$G_\chi = \frac{|g_l|^2}{m_\chi^2} \leq G_{\mathrm{F}}, \tag{19}$$

where $l = e, \mu, \tau$, and the value of G_{F} is taken from [17]. We shown in Figs. 4 and 5, the black curve shows this equality, and any value of $|g_l|^2$ and m_χ above this curve is stronger than its weak interaction.

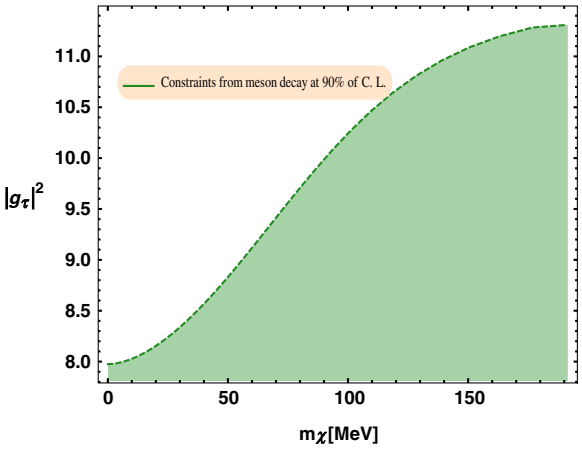

FIG. 6. Bounds on $|g_\tau|^2$ versus m_χ, the red curve comes from the meson decay at 90% C.L.

C. Higgs decay

One important consequence that may arise from the existence of low mass scalar particles is that it may induce invisible decays of the Higgs field. New LHC constrains such a decay at $\mathrm{Br}(h \to \text{invisible}) < 12\%$ [31–33].

In general, those invisible decays comes from couplings of the form

$$\mathcal{L} = -\frac{\lambda}{4}|H|^2|\chi|^2 \tag{20}$$

that allow three point interactions like $h|\chi|^2$ after symmetry breaking $H \to h + v$. This implies that $\lambda v \leq m_\chi$ and $\mathrm{Br}(h \to \chi\chi) \leq m_\chi^2/32\pi m_h$, which for current values of the Higgs mass and scalar mass sensitivity imply $\mathrm{Br}(h \to \chi\chi) < 0.47\%$, below the present experimental accuracy.

V. COMPARISON WITH NEUTRINO DECAY BOUNDS

This nonuniversal coupling can induce neutrino decays [3] that have an interesting phenomenology to make seasonal changes in the solar neutrinos rate [6] and affect neutrino oscillation behavior from long baseline experiments [4] such as MINOS [34] and T2K [35].

From Eq. (1) and assuming that the scalar mass is tiny enough, the mass eigenstate neutrinos can decay into one another during propagation via the decay $\nu_i \to \nu_j + \chi$. The neutrino lifetime from such a decay was computed by [36] assuming the third mass eigenstate to be much heavier than the light ones, $m_3 \gg m_{\mathrm{light}}$,

$$\frac{\tau_3}{m_3} = \frac{128\pi}{(\sum |g_{3j}|^2 + |h_{3j}|^2)m_3^2}. \tag{21}$$

The Ref. [4] analyzes MINOS and T2K experiments and compared the expected flux only from oscillated neutrinos and oscillated neutrinos plus decay to obtain a bound on the neutrino lifetime of $\tau_3/m_3 > 2.8 \times 10^{-12}$ s/eV at 90% C.L. Inserting this result in Eq. (21), the obtained bound can be translated to

$$\sum_{j=1,2} |g_{3j}|^2 + |h_{3j}|^2 < 3 \times 10^{-2}\left(\frac{\mathrm{eV}}{m_3}\right)^2, \tag{22}$$

where g and h are, respectively, the neutrino couplings in the mass basis with scalars and pseudoscalars. This limit is independent of a mass neutrino hierarchy between the states 2 and 3.

Another analysis taking into account the decay effects on solar neutrino data was performed by [6] whose neutrino life time obtained was $\tau_2/m_2 \geq 7.2 \times 10^{-4}\ \mathrm{s} \cdot \mathrm{eV}^{-1}$ at 90% C.L. which would give a bound of

$$|g_{21}|^2 + |h_{21}|^2 < 1.5 \times 10^{-5} \left(\frac{\text{eV}}{m_2}\right)^2 \tag{23}$$

at 90% C.L.

Our bounds listed in Tables IV and V are in a neutrino-scalar flavor basis. We can translate these bounds to a neutrino mass basis using the relation of Eq. (3). From the analysis of neutrino experiments [37], we can have the allowed range for the matrix elements of the mixing matrix U. First, we assume the bounds for $|g_e|^2$ and/or $|g_\mu|^2$ from Tables IV and V are valid, then

$$|g_{1j}|^2 < 3 \times 10^{-6}, \quad |g_{2j}|^2 < 4 \times 10^{-7}, \quad |g_{3j}|^2 < 5 \times 10^{-7}, \tag{24}$$

where $j = 1, 2, 3$; otherwise, if we assume that only the bounds on $|g_\tau|^2$ are valid, then the limits are much weaker: $|g_{1j}|^2 < 7 \times 10^{-3}$, $|g_{2j}|^2 < 2 \times 10^{-1}$, $|g_{3j}|^2 < 1 \times 10^{-1}$. The constraints from the neutrino decay in Eqs. (23) and (22) are dependent on the mass of the heavier neutrino mass eigenstate. For the degenerate mass scenario of $m_3 \sim m_2 \sim 1$ eV, the constraints from neutrino decay, in Eqs. (23) and (22) are always less restrictive then the results of this work, Eq. (24).

VI. CONCLUSION

We have computed the bounds for Yukawa interactions between Neutrinos and Hypothetical scalar particles χ using recent data and decay rates in two cases: (I) $m_\chi = 0$, obtaining the neutrino-scalar (pseudo-scalar) couplings in the flavor basis $|g_e|^2 < 1.9 \times 10^{-6}$, $|g_\mu|^2 < 1.9 \times 10^{-7}$ at 90% C.L., which is an improvement on previous results in literature and *for the first time*. And (II) $m_\chi \neq 0$ showing that those bounds for $\chi = 0$ can be safely used up to 100 MeV scale. Also no bounds can be put for masses $m_\chi \gtrsim 300$ MeV. For the mass basis the upper bound on neutrino-scalar couplings are $|g_{1j}|^2 < 3 \times 10^{-6}$, $|g_{2j}|^2 < 4 \times 10^{-7}$, and $|g_{3j}|^2 < 5 \times 10^{-7}$ which are much better then the indirect constrain from neutrino decay. In conclusion, there are no evidence for non-universal couplings between neutrino and scalar (pseudo-scalar).

We can conclude that we have no evidence for nonuniversal couplings between neutrino and scalar (pseudoscalar), and we get the best bounds from the meson decay rate and spectrum data.

ACKNOWLEDGMENTS

O. L. G. P thanks the hospitality of IPM-Iran and the support of FAPESP for the funding Grant No. 2012/16389-1. P. S. P. thanks also the support of FAPESP funding Grants No. 2014/05133-1 and No. 2015/16809-9 and the support of the Instituto de Física Corpuscular (CSIC-Universitat de València).

APPENDIX: IR TREATMENT

The differential rate given by Eq. (7) is infrared (IR) divergent, as can be seen by expanding it for small x and $m_\chi, \beta \to 0$,

$$d\Gamma(P \to l\nu_\alpha\chi) \overset{x\to\beta}{\to} \Gamma_0 \frac{|g_l|^2}{32\pi^2} \frac{1}{x} dx, \tag{A1}$$

which integrated goes as $\log(x)$ being divergent for the integration limits $0 < x < (1 - \sqrt{\alpha})^2$.

On the other hand, the correction of the neutrino propagator given by the diagram of Fig. 7 was calculated by Ref. [38] and changes the normalization of the neutrino field, δZ by,

$$\delta Z = -\frac{g^2}{32\pi^2} B_0(p; m_\chi, m_\nu), \tag{A2}$$

where B_0 is one of the Passarino-Veltman functions. This induces a change in the completeness relation,

$$\sum_s u(p,s)\bar{u}(p,s) = \not{p}(1 + \delta Z) + O(m_\nu), \tag{A3}$$

where p is the neutrino four momentum. Thus, one should add to the two-body decay $P \to l\nu_l$ the renormalization correction,

$$\Gamma(P \to l\nu) = \Gamma_0 \left(1 - \frac{|g_l|^2}{32\pi^2} B_0(p, m_\chi, m_\nu)\right). \tag{A4}$$

Expanding B_0 around a zero neutrino mass, one gets,

$$B_0(p, m_\chi, m_\nu) \overset{m_\nu\to 0}{\to} \log\left(\frac{E^2}{m_\chi^2}\right) = \log\left[\frac{(m_P^2 - m_l^2)^2}{4m_\chi^2 m_P^2}\right] \tag{A5}$$

but

$$\log\left[\frac{(m_P^2 - m_l^2)^2}{4m_\chi^2 m_P^2}\right] = \log\left[\frac{(m_P + m_l)^2}{4m_P^2}\right] + \int_\gamma^{(1-\sqrt{\alpha})^2} \frac{dx}{x}. \tag{A6}$$

Thus, summing both contributions, the $1/x$ is canceled at small m_χ due to opposite signs between the corrections in Eqs. (A1) and (A4).

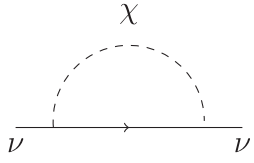

FIG. 7. Neutrino self-energy.

[1] V. D. Barger, W.-Y. Keung, and S. Pakvasa, Phys. Rev. D **25**, 907 (1982).
[2] A. P. Lessa and O. L. G. Peres, Phys. Rev. D **75**, 094001 (2007).
[3] G. T. Zatsepin and A. Y. Smirnov, Yad. Fiz. **28**, 1569 (1978) [Sov. J. Nucl. Phys. **28**, 807 (1978)].
[4] R. A. Gomes, A. L. G. Gomes, and O. L. G. Peres, Phys. Lett. B **740**, 345 (2015).
[5] J. M. Berryman, A. de Gouva, D. Hernndez, and R. L. N. Oliviera, Phys. Lett. B **742**, 74 (2015).
[6] R. Picoreti, M. M. Guzzo, P. C. de Holanda, and O. L. G. Peres, arXiv:1506.08158.
[7] T. Abrahao, H. Minakata, H. Nunokawa, and A. A. Quiroga, J. High Energy Phys. 11 (2015) 001.
[8] Y. Farzan, Phys. Rev. D **67**, 073015 (2003).
[9] J. Albert *et al.* (EXO-200 Collaboration), Phys. Rev. D **90**, 092004 (2014).
[10] K. Blum, A. Hook, and K. Murase, arXiv:1408.3799.
[11] L. Dorame, O. G. Miranda, and J. W. F. Valle, Front. Phys. **1**, 25 (2013).
[12] D. Cogollo, H. Diniz, C. de S. Pires, and P. Rodrigues da Silva, Eur. Phys. J. C **58**, 455 (2008).
[13] P. A. N. Machado, Y. F. Perez, O. Sumensari, Z. Tabrizi, and R. Z. Funchal, J. High Energy Phys. 12 (2015) 160.
[14] A. C. B. Machado and V. Pleitez, Phys. Lett. B **698**, 128 (2011).
[15] A. C. B. Machado and V. Pleitez, J. Phys. G **40**, 035002 (2013).
[16] A. Pilaftsis, Z. Phys. C **55**, 275 (1992).
[17] K. A. Olive (Particle Data Group), Chin. Phys. C **38**, 090001 (2014).
[18] W. J. Marciano and A. Sirlin, Phys. Rev. Lett. **71**, 3629 (1993).
[19] V. Cirigliano and I. Rosell, Phys. Rev. Lett. **99**, 231801 (2007).
[20] V. Cirigliano, G. Ecker, H. Neufeld, A. Pich, and J. Portoles, Rev. Mod. Phys. **84**, 399 (2012).
[21] G. B. Gelmini, S. Nussinov, and M. Roncadelli, Nucl. Phys. **B209**, 157 (1982).
[22] M. Ablikim *et al.* (BESIII Collaboration), Phys. Rev. D **89**, 051104 (2014).
[23] H.-B. Li, Nucl. Phys. B, Proc. Suppl. **233**, 185 (2012).
[24] J. P. Lees *et al.* (*BABAR* Collaboration) (2010).
[25] R. M. White (*BABAR* Collaboration), J. Phys. Conf. Ser. **347**, 012026 (2012).
[26] A. Zupanc *et al.* (Belle Collaboration), J. High Energy Phys. 09 (2013) 139.
[27] D. I. Britton *et al.*, Phys. Rev. D **46**, R885 (1992).
[28] A. V. Artamonov *et al.* (E949 Collaboration), Phys. Rev. D **91**, 052001 (2015); Phys. Rev. D **91**, 059903(E) (2015).
[29] S. Aoki *et al.*, Eur. Phys. J. C **74**, 2890 (2014).
[30] R. Trotta, Contemp. Phys. **49**, 71 (2008).
[31] J. Bernon, B. Dumont, and S. Kraml, Phys. Rev. D **90**, 071301 (2014).
[32] G. Belanger, B. Dumont, A. Goudelis, B. Herrmann, S. Kraml, and D. Sengupta, Phys. Rev. D **91**, 115011 (2015).
[33] C. Bonilla, J. W. F. Valle, and J. C. Romao, Phys. Rev. D **91**, 113015 (2015).
[34] P. Adamson *et al.* (MINOS Collaboration), Phys. Rev. Lett. **106**, 181801 (2011).
[35] K. Abe *et al.* (T2K Collaboration), Phys. Rev. Lett. **112**, 181801 (2014).
[36] C. W. Kim and W. P. Lam, Mod. Phys. Lett. A **05**, 297 (1990).
[37] M. C. Gonzalez-Garcia, M. Maltoni, and T. Schwetz, J. High Energy Phys. 11 (2014) 052.
[38] R. Schiopu, Ph.D. thesis, Mainz University, Inst. Phys., 2007.